

## Examination of Material Variation on the Life of Gas Turbine Backing-Up Renewable Energy Sources

Ezeddin Ali<sup>\*</sup>, Suresh Sampath, Pericles Pilidis, Saleh Mohammed

Department of Power and Propulsion, School of Aerospace, Transport and Manufacturing, Cranfield University, Cranfield, Bedfordshire, MK43 0AL, UK

<sup>\*</sup>Corresponding Author: Ezeddin Ali

---

**Abstract:** Gas turbine life and efficiency depend on the operating environment and material performance. Material selection is of prime importance to achieve high life and efficiency. This paper focuses on the study of the effect of material properties and variation in alloy composition of a high-pressure turbine blade on gas turbine life when works in the flexible mode as a pick-up of renewable sources. A tool has been developed wherein different scenarios can be simulated to obtain engine life consumption factors. The engine life is examined according to the different material for different operating scenarios. It is observed that blade life is highly affected by changing material properties and moreover it is noted that the small change in the mass percentage of some constituent elements of an alloy results in a significant difference in HPT blade life.

**Keywords:** Renewable Energy; Flexibility; Power Demand; Gas Turbines; Creep-LCF life; Material Properties ; Material composition

---

Date of Submission: 31-01-2019

Date of acceptance: 16-02-2019

---

### I. Introduction

Gas turbine components need to operate under the most arduous conditions of a significant rotational and gas bending stresses at extremely high temperature, in addition to thermomechanical loading cycles as a result of start-up and shutdown operation. This situation makes gas turbine blades prone to different failure modes such as creep damage, fatigue damage, environmental attack (oxidation, sulphidation, hot corrosion) and combined failure mechanism which lead to weaken and limit the performance of the blades[1].

The prime design criteria for gas turbine blades are creep and oxidation resistance. The blades are manufactured from special alloys which mainly include iron, nickel, cobalt and chromium with an addition of about ten significant alloying elements[2]. The most widely used alloys are Nimonic alloy and Inconel. These alloys are Nickel based which can hold their strength even at high temperatures. Nickel-based superalloys are excellent high-temperature materials and have proven very useful. Aluminium and titanium are the essential solutes in nickel-based alloys, with less than 10% of a total concentration. The chemical additions of aluminium and titanium promote the creation of the gamma prime  $\gamma'$  phase which acts as a barrier to dislocation motion. This phase is responsible for the high-temperature resistance and high creep deformation resistance of the material alloy[3]. Cobalt-based superalloys potentially possess superior hot corrosion, oxidation, and wear resistance. The microstructure of alloys consists of small grains stacked in a regular array with a boundary layer between them to hold them together. Addition of different elements to alloy such as Aluminium, Titanium, Tungsten, and Rhenium used to increase the precipitate hardening and substitution strengthening which increase the creep strength. Each of these additions has been chosen to serve a particular purpose in optimizing the properties for the high-temperature application. Chromium is also used in Nickel and Cobalt based super alloys as it provides oxidation and corrosion resistance.

The improvements in alloy strength have been attained by increasing the refractory elements and decreasing the chromium content. Developing new low-density alloys for the turbine blade application have a significant improvement in the thrust to weight ratio and lead to decrease stresses produced from the centrifugal force arising from shaft rotation.

The preferred blade element is Nickel-based superalloy which has nickel as the primary element rather than Co or Fe-based superalloys. It has significant characteristics of high strength, creep resistance at high temperature, corrosion and oxidation resistance, and good surface stability. It has a wide range of application in the manufacture of a gas turbine for use in aircraft engines, power production and marine propulsion[4].

Different generations of superalloys have been developed tending to have higher temperature resistance. The characteristics of alloys are different depending on chemical composition and on the percentage of refractory elements. Superalloys consist of different alloying elements with different percentages. One of the most famous families of superalloys is Nimonic alloys, which are made using more than 50% of nickel and 20%

of chromium with the addition of small amounts of titanium and aluminium. Another family of superalloys is the Inconel alloys, which usually consist of nickel, chrome and some iron [5]. Some of the materials percentage in superalloys are not given accurately in the open-source literature. For example, the composition of Nickel-based Nimonic alloy 115 as shown in Table 1 has a variation in some material mass percentage such as Titanium and Aluminium.

**Table 1.** Nominal Composition % of NIMONIC alloy 115

Carbon .....	0.12-0.2
Silicon .....	1.0 max
Copper .....	0.2 max
Iron .....	1.0 max
Manganese .....	1.0 max
Chromium .....	14.0-16.0
Titanium .....	3.5-4.5
Aluminium .....	4.5-5.5
Cobalt .....	13.0-15.5
Molybdenum .....	3.0-5.0
Boron .....	0.01-0.025
Zirconium .....	0.15 max
Lead .....	0.0015 max
Sulfur .....	0.015 max
Nickel .....	Balance*

Single crystal superalloys have wide application in manufacturing turbine blades due to its unique combination of properties and performance. It incorporates expensive new rare alloying elements such as rhenium and ruthenium to achieve the desired characteristics. Examples of single crystal superalloys such as CMSX-4 and Rene N5 which containing 3% of Rhenium, and it have the greatest market utilization. Creep strength amelioration in superalloys have been achieved by increases in dense refractory elements such as rhenium and tungsten but this increases the blade weight and cascades to the disk and shaft. Superalloys with high densities can limit the use of superalloy, in addition to the high cost of these elements. Consequently, new single crystal superalloys are developed with lower rhenium content such as CMSX-7 and CMSX-8[6].

According to the material properties and their effect on GT blade life, this study aims to estimate the life consumption due to the superposition of creep and fatigue failure on high-pressure turbine blade as a result to small variation in the mass percentage of alloy materials. As a part of the research, a tool has been developed which has the capability of giving an estimate of how much life is being consumed for load-following plants used during seasonal operations.

## II. Case study

An intercooler two shaft aero-derivative gas turbine engine of 100MW has been selected as a case study with performance parameters as shown in table 2. The effect of creep-fatigue interaction on the high-pressure turbine (HPT) blade when operating in flexible mode was studied, the reason for choosing HPT blade is due to its exposure to the harsh environment (high temperatures) and high stresses. The effect of the material was examined on six different material alloys used for turbine blades based on the data available in the literature. Estimate of creep-fatigue life consumption of HPT blade leads to a reasonable assessment of the gas turbine life. The creep-fatigue life prediction for HPT blade has been carried out according to the material properties including physical properties, tensile properties and creep properties. Three types of Nimonic alloys are selected (Nimonic alloy-90, Nimonic alloy-105 and Nimonic alloy-115)[7][8][9] and two types of Inconel alloys (Inconel-718 and Inconel-738LC)[10][11][12], by addition to one single crystal superalloy (CMSX-8)[6]. The material properties are gathered from open source literature including; density, Young's modulus, tensile strength and Larson Miller parameter.

**Table 2.** Engine performance data

Parameter	Value	Unit
Power output	100	MW
TET	1630	K
Efficiency	44.8	%
RPM	9300	Rev/min
Fuel Flow	4.9011	Kg/sec
Mass flow	216.5	Kg/sec
Pressure ratio	42	

### III. Methodology

The investigations were done for HPT blade material to examine the effect of material properties on gas turbine life. Different materials used in gas turbine blades are chosen to check their properties in engine life. Furthermore, the material alloy composition investigates to know its influence in the engine life. The gas turbine was simulated to work according to different scenarios of variable ambient temperature and power demand (Fig.1 and 2). These scenarios were created based on 2016 daily data collected from Weatherbase data[13] and UK National grid status [14] for ambient temperature and power demand respectively. The data are gathered for every hour and classified into four seasons. The daily temperature and power production are represented by the average calculated for each season.

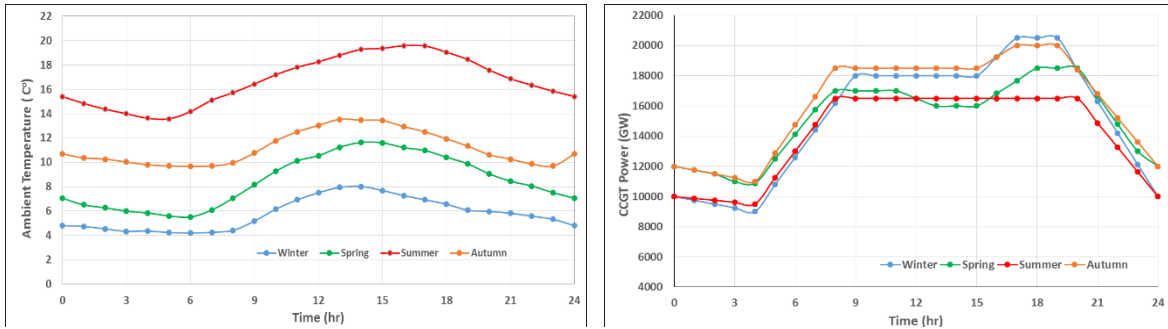


Figure 1. UK daily average ambient temperatures (2016) Figure 2. UK daily average CCGT power production (2016)

An algorithm has been developed in FORTRAN 95 according to the methodology shown in Fig.3, which includes many modules; Performance simulation Module, stress module, thermal module and creep-fatigue life module. Performance simulation has been carried out using In-House software TURBOMATCH (Appendix 1) developed at Cranfield University. TURBOMATCH uses input data for every season to simulate engine performance. Its results are used for stress and thermal modules.

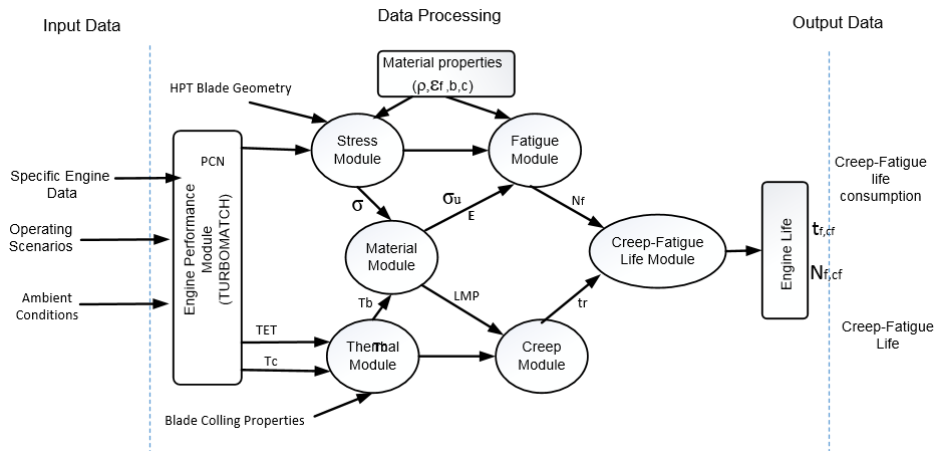


Figure 3. Life Simulation Methodology

Thermal module is used to define the temperature of HPT blade every hour according to the daily operating scenario. A simple and flexible 0D model for uniform temperature distribution on the blade is used. This module requires turbine entry temperature (TET), blade cooling air temperature (Tc) and blade cooling effectiveness (ε), assuming (ε) of 0.637 according to the type of blade cooling[15]. Then the blade material temperature is calculated by Equation (1):

$$T_b = TET - \varepsilon(TET - T_c) \quad (1)$$

Gas turbine blades experience a high level of stresses arising from centrifugal loads, gas bending moments and thermal stresses during its operation. Some assumptions were made to eliminate the complications regarding input data used in this model due to the lack of information about accurate blade geometry and gas properties. It was assumed that the axial velocity remains constant along the span of the blade and the centrifugal force acts at the centre of the blade section. Due to the mass of the blade and the fact that about 80% of material strength consumed by centrifugal stress which considered as the main prevalent stress[16]. Only centrifugal stress is considered in the stress module which arises from the mass blade, and it is a function of blade rotational speed (PCN). The maximum stress due to centrifugal force was calculated using Equation (2):

$$\sigma_{max} = \frac{\rho\omega^2}{2}(R_t^2 - R_r^2) \quad (2)$$

Where:  $\sigma$  = applied stress  
 $R_t$  = Radius of the blade root from the rotation axis  
 $R_c$  = Radius of the blade tip from the rotation axis  
 $\rho$  = material density  
 $\omega$  = Radial rotational speed =  $\frac{2\pi N}{60}$

Output data for both thermal and stress module use as input in material properties module to calculate Larson Miller parameter (LMP) for creep life calculation (Appendix 2), and mechanical properties of blade material for low-cycle fatigue (LCF). The time to failure due to creep was estimated using Equation (3):

$$t_f = 10 \left( \frac{1000 LMP}{T} - C \right) \quad (3)$$

Coffin- Manson method and Neuber's constant for stress concentration (Appendix 3) was used for estimating the number of cycles to failure in fatigue module using Equation (4):

$$\frac{\Delta\varepsilon}{2} = \frac{\sigma'_f}{E} (N_f)^b + \varepsilon'_f (N_f)^c \quad (4)$$

From the creep-fatigue life module including creep life module and LCF life module, daily creep-fatigue life consumption for all scenarios was calculated using the linear damage summation method. This method widely used because it requires only standard S-N curves and stress-rupture curves and it is easy to use [17], while other methods involve many parameters and constants which are difficult to determine or need additional tests to obtain. Linear damage summation method is simplified and good for the objective of the comparative study. It combines the damage summations of Robinson's rule for creep and the Palmgren-Miner's rule for fatigue. It is based on the concept that fatigue damage is surface phenomenon while creep damage is an internal process of initiation and propagation of cracks between grains boundaries. The total damage is the summation of life fraction for the fatigue damage ( $D_f$ ) and life fraction for the creep damage ( $D_c$ ).

$$D_{cf} = D_c + D_f \quad (5)$$

Where  $D_f = \sum \frac{N_i}{N_f}$  and  $D_c = \sum \frac{t_i}{t_f}$  and it is expressed as:

$$\sum \frac{t_i}{t_f} + \sum \frac{N_i}{N_f} = D_{c+f} \quad (6)$$

Where  $t_i$  -time spent at given stress (one hour)  
 $t_f$  -time to rupture at stress-temperature combination corresponding to  $\sigma$   
 $N_i$  -Number of cycles per day  
 $N_f$  -Number of cycles to failure at stress amplitude  $\sigma$

The value of D display the damage level of the material component, and it is assumed that the failure occurs when it is equal to one.

The life estimation is done for every selected material according to material properties including material density, Young's modulus, ultimate strength, yield strength, and Larson Miller parameter. Coffin-Manson's parameters shown in Table 3 are selected based on averaged parameters method proposed by Meggiolaro and Castro [18], which uses the median values of each of these parameters estimated for different alloy family including steels, aluminium, titanium and nickel alloys [19].

**Table 3.** Coffin-Manson's parameters

Parameter	Value
$\sigma'_f$	$1.4\sigma_u$
$\varepsilon'_f$	0.15
$b$	-0.08
$c$	-0.59

Based on the mentioned earlier in section 1 about the variation in alloy materials percentage. Nickel-based Nimonic alloy 115 was selected for this study to examine the effect of changing some elements percentage on gas turbine blade life. The nominal composition of Nimonic 115 is shown in Table 1 [9].

The mass percentage of some elements given in literature is not precise such as Titanium which ranges between 3.5 and 4.5. In order to calculate the density of the alloy from the individual density of its components, the average of these elements percentage was taken and then the density of the alloy was calculated. The result gives a different value. The alloy has a relatively complex microstructure, it does not make sense to estimate the density of a solid solution from the density of the components unless each component has the same crystal structure of the final solid solution and all of them have similar size. And more, even in the last case, there may be subtle effects such as ordering, introducing significant deviation from a supposedly linear correlation

between density and composition. However, it gives an idea about the effect of change of material composition on the material life.

The new density value is taken as a reference (7.39 g/cm<sup>3</sup> rather than real value 7.85 g/cm<sup>3</sup>). The mass percentage of some light material (Aluminium and Titanium) was increased by 0.5%, 1% and maximum percentage, also it was decreased by 0.5%, 1%, and the minimum percentage. The change in alloy mass percentage was compensated by add and subtract the same amount of heavy material (Chromium and Cobalt). The volume of every element is calculated according to its density, then the alloy density was calculated from the whole mass and volume of the alloy by using Equation (7):

$$\text{Density} = \text{mass} / \text{volume}. \tag{7}$$

## IV. Results and Discussions

### 1.1. Seasonal operating scenarios

According to the data collected for CCGT power production and ambient temperature for the UK during 2016, the seasonal operating scenarios in Fig.7 have been created for the 100MW gas turbine. Performance simulation has been done using In-house software TURBOMATCH to estimate the main factors affecting creep life and low cycle fatigue life. A separate computer code was developed in FORTRAN 95 utilizing the performance parameters from a simulation of the different scenarios to determine the creep-fatigue life prediction for HPT blade.

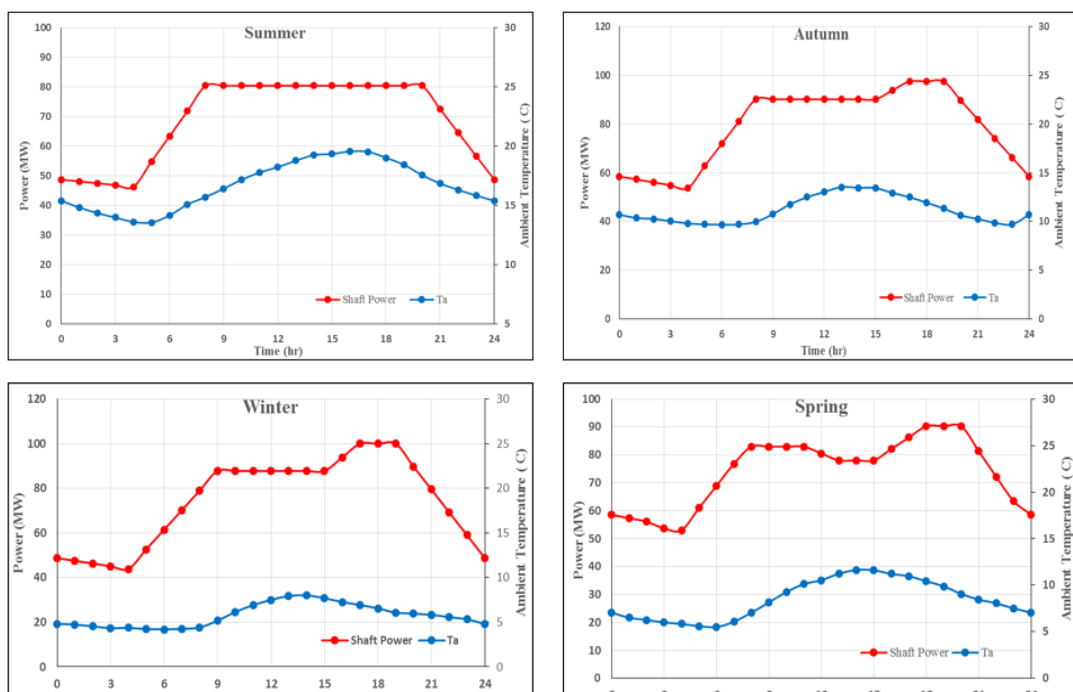


**Figure 7.** Seasonal daily operating scenario

### 1.2. Gas turbine life for different alloys

The results show the variation in life consumption according to the different failure mechanism (creep, LCF and creep-fatigue failure) during different operating scenarios. The daily life consumption for all selected alloys are shown in Fig.8.

Autumn has the highest life consumption for alloys due to the higher power demand and high ambient temperature compared with other seasons. Summer has the lowest life consumption despite its higher ambient temperature compared with other seasons due to lower power demand. It is notable that from the whole life consumption during one year that the Inconel 718 and Nominic 90 have very high creep life consumption compared with other alloys (Fig. 9). The lowest creep life consumption was recorded by CMSX-8 and Nominic 115. As shown in table 4, it is clear that when the density of the nickel-based alloy material decreased, the engine life increased. Although single crystal material has higher density compared with nickel-alloys, it has a longer life. That is due to its unique combination of properties and performance, and there is no grain boundary in the material where the creep can precipitate.

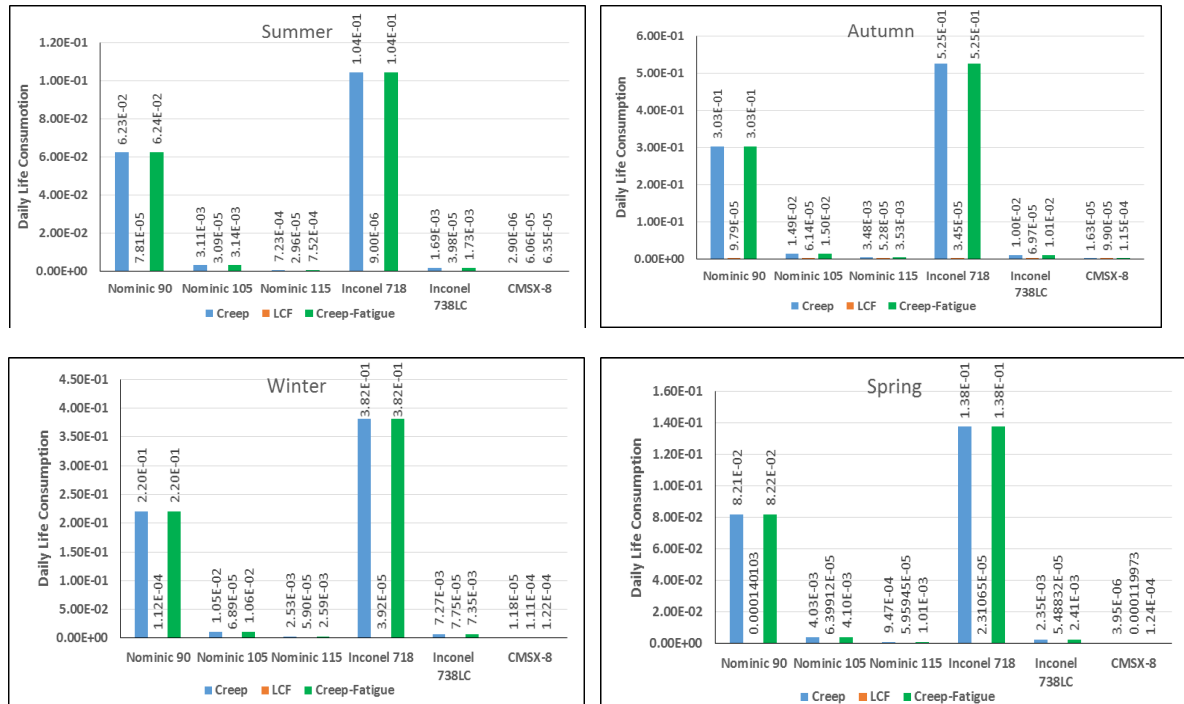


Figure (8) Daily life Consumption for selected alloys

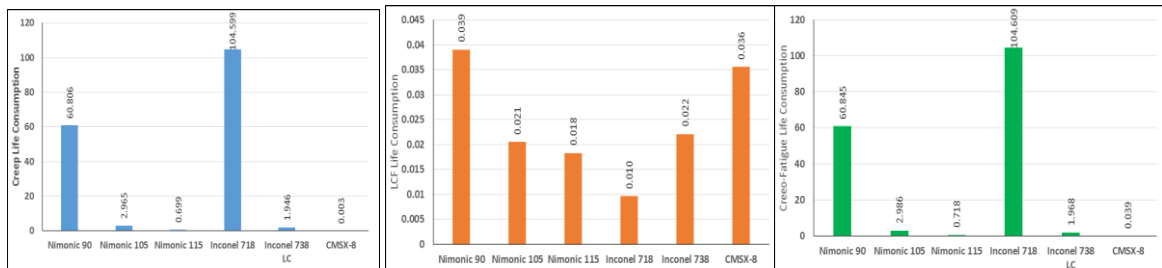


Figure (9) Annual creep life consumption Figure (10) Annual LCF life consumption Figure (11) Annual creep-fatigue life consumption

Fig.10 illustrate that the annual LCF life consumption is very small compared with creep life consumption when the engine working in this mode of operation. The highest LCF life consumption occurs for Nimonic 90, while the lowest LCF recorded by Inconel 718.

The results show that Inconel 718 can withstand and resist the effect of cycling operation very much compared with other alloys, but it is very week against creep failure.

Inconel 718 and Nimonic 90 have higher values of creep-fatigue life consumption (Fig.11), the other alloys are more suitable to have higher life when working in flexible mode operation as shown in Table4.

Table 4. Creep-Fatigue life of different material

Alloy	Density (kg/m <sup>3</sup> )	Creep Life (day)	LCF Life (cycle)	Creep-Fatigue Life (day)	Creep-Fatigue life (hour)
Inconel 718	8221	3.49	37877.96	3.49	83.74
Nimonic 90	8180	6.00	9361.60	6.00	143.97
Inconel 738LC	8110	187.59	16555.48	185.48	4451.61
Nimonic 105	8010	123.09	17786.39	122.24	2933.75
Nimonic 115	7850	521.98	19921.61	508.66	12207.73
CMSX-8	8850	114653.19	10263.79	9420.47	226091.36

### 1.3. Effect of material composition on GT life

The results illustrate that the gas turbine blade life is highly affected by the change in material density. According to that, the effect of material composition was investigated using Nimonic 115 as a case study to check the effect of a change in some elements percentage on gas turbine blade life.

The mass percentages of some light material (Aluminium and Titanium) are increased and decreased by small values as instant shown in Table5. The aluminium and titanium percentage increased by 1% and Chromium and

Cobalt decreased by the same percentage. The density of alloy becomes  $7.3 \text{ g/cm}^3$ ; this value was used to calculate blade life. This change has a significant effect on material life; the creep-fatigue life increased by more than 1000 Hours and vice versa as shown in Table 5. Fig.12 shows that there is a big difference in engine life when the percentage of light material changes from a minimum amount to maximum. The blade life increased by more than 2300 hours.

**Table 5.** Effect of change of alloying element density on GT blade life

Alloy Density ( $\text{g/cm}^3$ )	Calculated Density ( $\text{g/cm}^3$ )	Mass %	Creep Life $t_{r_c}$ (days)	LCF Life $N_f$	Creep-Fatigue life $t_{r_{cf}}$ (days)	Creep-Fatigue life $t_{r_{cf}}$ (hours)
7.7379	7.1891	Max % of light material (Al+Ti)	448.26	18272.0	437.53	10500.7
7.7536	7.2037	1% increase of light material (Al+Ti)	440.8	18034.0	430.29	10326.86
7.8015	7.2482	0.5% increase of light material (Al+Ti)	417.86	17474.0	408.10	9794.40
7.85	7.2933	mean	395.82	16939.0	386.79	9282.84
7.8991	7.3389	0.5% decrease of light material (Al+Ti)	375.10	16344.0	366.68	8800.34
7.9488	7.3851	1% decrease of light material (Al+Ti)	355.21	15856.0	347.43	8338.2
7.9654	7.4005	Min % of light material (Al+Ti)	349.10	15661.0	341.49	8195.71

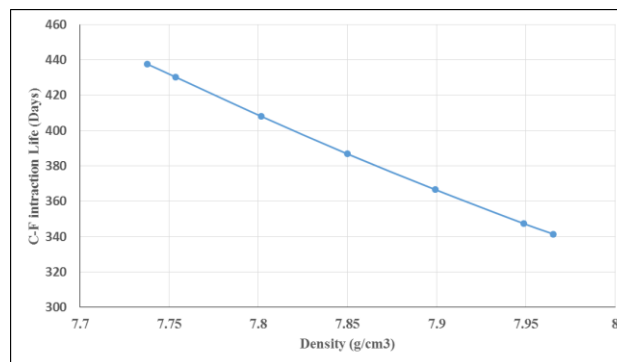


**Figure 12.** Effect of change material density on GT life

This investigation gives an idea about how the small change in the alloying element has a big effect on gas turbine blade life.

### V. Conclusion

This paper attempts to provide an analytical view of the effect of material properties and composition on gas turbine blade life working under flexible operating mode. Some of the findings of the research are listed below:

- Blade life differs from material to other depending on material properties.
- Blade life is highly affected by material density, the life decrease by increase material density.
- According to flexible mode, the LCF life consumption is very small compared with creep life consumption.
- Blade life differs with alloy composition.
- The small change in the mass percentage of constituent elements of alloy components results to a significant difference in blade life.

### References

- [1]. I. A. Essienubong, O. Ikechukwu, P. O. Ebnilo, and E. Ikpe, "Material Selection for High Pressure (HP) Turbine Blade of Conventional Turbojet Engines," *Am. J. Mech. Ind. Eng.* Ikpe Aniekan Essienubong *Am. J. Mech. Ind. Eng.*, vol. 1, no. 1, pp. 1–9, 2016.
- [2]. S. K. Bohidar, R. Dewangan, and P. K. Kaurase, "Advanced materials used for different components of Gas Turbine," vol. 1, no. 7, pp. 366–370, 2013.
- [3]. A. Kracke, "Superalloys, the Most Successful Alloy System of Modern Times-Past, Present, and Future," 7th Int. Symp. Superalloy 718 Deriv., pp. 13–50, 2010.
- [4]. M. Segersäll, Nickel-Based Single-Crystal Superalloys temperature properties, no. 1568. 2013.
- [5]. & D. S. & S. P., "INSG Insight," Alloy. Nickel-based Superalloy, no. 20, pp. 1–9, 2013.
- [6]. J. B. Wahl and K. Harris, "New single crystal superalloys, CMSX®-7 and CMSX®-8," *Proc. Int. Symp. Superalloys*, pp. 179–188, 2012.
- [7]. M. Range, "NIMONIC alloy 90," vol. 90, no. 2, 1975.
- [8]. W. Nr, "NIMONIC alloy 105," vol. 115, no. 2, pp. 3–6, 2003.
- [9]. W. Nr, "NIMONIC alloy 115," vol. 115, no. 2, pp. 3–6, 2003.
- [10]. Special Metals, "INCONEL alloy 718," pp. 1–28, 2007.
- [11]. B. George and J. J. Galka, "Alloy IN-738 Technical Data," Int. nickel company, INC., 1969.
- [12]. A. K. Koul, R. Castillo, and K. Willett, "Creep life predictions in nickel-based superalloys," *Mater. Sci. Eng.*, vol. 66, no. 2, pp. 213–226, 1984.
- [13]. WU, "Weather history and data archive." <https://www.wunderground.com/history/>.
- [14]. Gridwatch, G.B. National Grid Status. UK: <http://www.gridwatch.templar.co.uk>, 2016.



- [15]. B. L. Koff, "Gas Turbine Technology Evolution: A Designers Perspective," J. Propuls. Power, vol. 20, no. 4, pp. 577–595, 2004.
- [16]. W. Mohamed, S. Eshati, P. Pilidis, S. Ogaji, P. Laskaridis, and a Nasir, "A method to evaluate the impact of power demand on HPT blade creep life," vol. 4, pp. 1–9, 2011.
- [17]. M. H. Sabour and R. B. Bhat, "Lifetime Prediction in Creep-Fatigue Environment," Ind. Eng., vol. 26, no. 3, pp. 1–15, 2008.
- [18]. M. A. Meggiolaro and J. T. P. Castro, "Statistical evaluation of strain-life fatigue crack initiation predictions," Int. J. Fatigue, vol. 26, no. 5, pp. 463–476, 2004.
- [19]. V. T. T. and L. A. Khamaza, "STRAIN-LIFE CURVES OF STEELS AND METHODS FOR DETERMINING THE CURVE PARAMETERS," vol. 42, no. 6, 2010.
- [20]. R. A. Cookson and A. S. Haslam, "Fatigue and Fracture," in MSc in Thermal Power Lecture Notes, Cranfield, Bedfordshire, UK: Cranfield University, 2013.
- [21]. S. P. Saravanamuttoo, H. H. Rogers, G. F. C. Cohen, H. Gas Turbine Theory, SIXTH EDITION, 2009.

## Appendix A TURBOMATCH

TURBOMATCH is a performance simulation software developed by Cranfield University. It is capable of performing design, off-design and transient operation of any gas turbine configuration. This program has been used for academic research and has proven a very powerful, reliable, accurate and flexible tool for engine performance simulation.

## Appendix B CREEP MODULE

Larson Miller approach used to calculate the time to failure ( $t_f$ ) due to creep according to stress and blade temperature by using the following Equation:

$$LMP = \frac{T}{1000} (\log t_f + C) \quad (\text{B-1})$$

Creep Life (hours):

$$t_f = 10 \left( \frac{1000LMP}{T} - C \right) \quad (\text{B-2})$$

$$\text{Creep life consumption per hour} = \frac{1}{t_f} \quad (\text{B-3})$$

Where:  $LMP$  - Material Larson-Miller Parameter

$T$  - Absolute operating temperature (K)

$t_f$  - Time to rupture (hour)

## Appendix C LOW CYCLE FATIGUE MODULE

Coffin- Manson method and Neuber's constant for stress concentration was used to estimating the number of cycles to failure in fatigue module according to the following equations [20]:

$$\sigma_a = \sigma_{max} \times \text{Stress concentration factor} \quad (\text{C-1})$$

$$\varepsilon_a = \frac{\sigma_a}{E} \quad (\text{C-2})$$

$$\text{Neuber's constant} = \sigma_a \times \varepsilon_a \quad (\text{C-3})$$

$$\text{Neuber's constant} = \sigma_b \times \varepsilon_b \quad (\text{C-4})$$

$$\varepsilon_b = \frac{\sigma_b}{E} + \left( \frac{\sigma_b}{K'} \right)^{\frac{1}{n'}} \quad (\text{C-5})$$

$$K' = \frac{\sigma_f}{(\varepsilon'_f)^{n'}}, \quad n' = \frac{b}{c} \quad (\text{C-6})$$

Where:  $\sigma_a$  = Applied stress at stress concentration zone.

$\varepsilon_a$  = Strain resulted at stress concentration zone

$E$  = Modulus of elasticity

$\sigma_b, \varepsilon_b$  = cyclic maximum stress and strain respectively

$K'$  = cyclic strength coefficient

$\sigma_f$  = fatigue strength coefficient

$\varepsilon'_f$  = fatigue ductility coefficient

$n'$  = cyclic strain hardening exponent

$b$  = fatigue strength exponent

$c$  = fatigue ductility exponent

For the majority of materials,  $b$  varies from -0.5 to -0.12 and  $c$  varies from -0.5 to -0.7 [20][21].

By solving Eqs. (C.4) and (C.5)  $\sigma_b$  and  $\varepsilon_b$  can be defined. The behaviour of cyclic unloading:

$$\text{Neuber's constant} = \Delta\sigma \times \Delta\varepsilon \quad (\text{C-7})$$

$$\Delta\varepsilon = \frac{\Delta\sigma}{E} + 2 \left( \frac{\Delta\sigma}{2K'} \right)^{\frac{1}{n'}} \quad (\text{C-8})$$



Where:  $\Delta\sigma$  and  $\Delta\varepsilon$  Cyclic stress variation and cyclic strain variation respectively  
 $\Delta\sigma$  and  $\Delta\varepsilon$  can be defined by solving Eqs. (C.7) and (C.8), by a substitute in Coffin-Manson strain life equation, the number of cycle to failure ( $N_f$ ) can be found:

$$\frac{\Delta\varepsilon}{2} = \frac{\sigma'_f}{E} (N_f)^b + \varepsilon'_f (N_f)^c \quad (\text{C-9})$$

The Morrow's mean stress life Equation:

$$\frac{\Delta\varepsilon}{2} = \frac{(\sigma'_f - \sigma_m)}{E} (2N_f)^b + \varepsilon'_f (2N_f)^c \quad (\text{C-10})$$

Patrick Wamalwa. "Examination of Material Variation on the Life of Gas Turbine Backing-Up Renewable Energy Sources." IOSR Journal of Mechanical and Civil Engineering (IOSR-JMCE) , vol. 16, no. 1, 2019, pp. 60-68

# Examination of material variation on the life of gas turbine backing-up renewable energy sources

Ali, Ezeddin

2019-02-28

Attribution-NonCommercial 4.0 International

---

Ali E, Sampath S, Pilidis P, Mohamed S. (2019) Examination of material variation on the life of gas turbine backing-up renewable energy sources. IOSR Journal of Mechanical and Civil Engineering, Volume 16, Issue 1, Jan-Feb 2019, pp. 60-68

<https://doi.org/10.9790/1684-1601046068>

*Downloaded from CERES Research Repository, Cranfield University*